Numerical modeling and sensitivity analysis of seawater intrusion in a dual-permeability coastal karst aquifer with conduit networks

Zexuan Xu[1, *], Bill X. Hu[2] and Ming Ye[3]

[1]Climate and Ecosystem Sciences Division, Lawrence Berkeley National Laboratory, Berkeley, California, 94720, USA

[2]Institute of Groundwater and Earth Sciences, Jinan University, Guangzhou, Guangdong, China

[3]Department of Scientific Computing, Florida State University, Tallahassee, Florida, 32306, USA

*Corresponding author: email address: xuzexuan@gmail.com;

Submitted to Hydrology and Earth System Sciences

Abstract

Long distance seawater intrusion is widely observed through the highly permeable subsurface conduit system, and contaminates groundwater resources in coastal karst aquifers. In this study, a two-dimensional density-dependent flow and transport SEAWAT model is created to study seawater intrusion in the dual-permeability karst aquifer with conduit networks. To understand seawater intrusion in such an aquifer, local and global sensitivity analysis are used to evaluate the effects of boundary conditions and hydrological characteristics, including hydraulic conductivity, effective porosity, specific storage and dispersivity of the conduit and the porous medium on modeling simulations. The local sensitivity evaluates the parameters sensitivities specifically for modeling seawater intrusion in the WKP. The global sensitivity analysis provides a more comprehensive interpretation of parameter sensitivities within the ranges, due to the non-linear relationship between simulations and parameters. The conduit parameters are important to the simulations in the porous medium, because of the interaction between the two systems. Therefore, salinity and head simulations in the karst features, such as the conduit system and submarine springs, are critical for understanding seawater intrusion in a coastal karst aquifer. In the continuum SEAWAT model, Darcy's equation does not accurately compute the conduit flow velocity by head difference and hydraulic conductivity. In addition, dispersivity is no longer an important parameter in advection-dominated karst aquifer with conduit system, compared to the sensitivity results in a porous medium aquifer. Finally, the extents of seawater intrusion are quantitatively evaluated under the scenarios of changing the important parameters identified from

sensitivity results, including salinity at the submarine spring with rainfall recharge, sea level rise and longer simulation time under an extended low rainfall period.

Key Words: Seawater intrusion; Coastal karst aquifer; Variable-density numerical model; Dual-permeability karst system; Sensitivity analysis

1. Introduction

50   Many serious environmental issues have been caused by seawater intrusion in the coastal regions, such as soil salinization, marine and estuarine ecological changes, and groundwater contamination (Bear, 1999). Werner et al. (2013) pointed out that climate variations, groundwater pumping, and fluctuating sea levels are important factors to the mixing of seawater and freshwater in the aquifer. Custodio (1987) and Shoemaker (2004)

55   summarized the control factors of seawater intrusion into a coastal aquifer, including the geologic and lithological heterogeneity, localized surface recharge, paleo-hydrogeological conditions and anthropogenic influences. Meanwhile, seawater intrusion in a coastal aquifer is significantly impacted by sea level rise, which has been recognized as a serious environmental threat in this century (Voss and Souza, 1987; Bear, 1999;

60   IPCC, 2007). The Ghyben-Herzberg relationship presents that a small rise of sea level would cause extended seawater intrusion, and significantly moves the mixing interface position further landward in a coastal aquifer (Werner and Simmons, 2009). Essink et al. (2010) pointed out that seawater intrusion is exacerbated under sea level rise and global climate change. Likewise, high tides associated with hurricanes or tropical storms have

65   been found to temporarily affect the extent of seawater intrusion in a coastal aquifer

(Moore and Wilson, 2005; Wilson et al., 2011).

Modeling seawater intrusion in a coastal aquifer requires a coupled density-

dependent flow and salt transport groundwater model. The solution of salinity simulation

is computed by the groundwater velocity field from flow modeling, and salinity in turn

70   determines water density and affects the simulation of flow field. Several variable-density

numerical models have been developed and widely used to study seawater intrusion,

including SUTRA (Voss and Provost, 1984) and FEFLOW (Diersch, 2002). SEAWAT is

a widely used density-dependent model, which solves flow equations by finite difference

method, and transport equations by three major classes of numerical techniques (Guo and

75   Langevin, 2002; Langevin et al., 2003). Generally speaking, most variable-density

models are numerically complicated and computational expensive, with smaller timestep

and implicit procedure of solving flow and transport equations iteratively many times in

each timestep (Werner et al., 2013).

On the other hand, a karst aquifer is particularly vulnerable to groundwater

80   contamination including seawater intrusion in a coastal region, since the well-developed

sinkholes and karst windows are usually connected by highly permeable subsurface

conduit networks. Some karst caves are found open to the sea and become submarine

springs below the sea level, connected with the conduit network as natural pathways for

seawater intrusion. Fleury et al. (2007) reviewed the studies of freshwater discharge and

85   seawater intrusion through karst conduits and submarine springs in coastal karst aquifers,

and summarized the important control factors, including hydraulic gradient of equivalent

freshwater head, hydraulic conductivity, and seasonal precipitation variation. For

example, preferential flow within a conduit significantly intrudes landward and contaminate the groundwater in a coastal karst aquifer (Calvache and Pulido-Bosch,

90   1997). As an indicator of rainfall and regional freshwater recharges, salinity at the outlet of conduit system is diluted by freshwater discharge during a rainfall season, but remains constant as saline water during a low rainfall period (Martin and Dean, 2001; Martin et al., 2012).

        Modeling groundwater flow in a dual-permeability karst aquifer is a challenging

95   issue since groundwater flow in a karst conduit system is often non-laminar (Davis, 1996; Shoemaker et al., 2008; Gallegos et al., 2013). Several discrete-continuum numerical models, such as MODFLOW-CFPM1 (Shoemaker et al., 2008) and CFPv2 (Reimann et al., 2014; Reimann et al., 2013; Xu et al., 2015a; Xu et al., 2015b), have been developed to simultaneously solve the non-laminar flow in the conduit, the Darcian flow in a porous

100   medium and the exchanges between the two systems. However, these constant-density karst models are not applicable to simulate the density-dependent seawater intrusion processes in a coastal aquifer. Recently, the VDFST-CFP developed by Xu and Hu (2017) is a density-dependent discrete-continuum modeling approach to study seawater intrusion in a coastal karst aquifer with conduits. However, VDFST-CFP is not able to handle the

105   issues addressed in this study, because of the computational constraints associated with the aquifer geometry and the domain scale. For more details, please refer to Xu and Hu (2017). Therefore, the variable-density SEAWAT model is still applied in this study, in which Darcy equation is used to compute flow not only in the porous medium, but also in the conduit with large values of hydraulic conductivity and effective porosity.

110   Several sensitivity studies have evaluated the parameters in karst aquifers. Kaufmann and Braun (2000) reported that boundary conditions and sink recharges are important to the preferential flow path in a karst aquifer. Scanlon et al. (2003) also confirmed that recharge is important to karst spring discharge. Very few studies have addressed the parameter sensitivities of seawater intrusion in a coastal karst aquifer.

115   Shoemaker (2004) performed a sensitivity analysis of the SEAWAT model for seawater intrusion to a homogeneous porous aquifer, concluded that dispersivity is an important parameter to the head, salinity and groundwater flow simulations and observations in the transition zone. Shoemaker (2004) also concluded that salinity observations are more effective than head observation, and the "toe" of the transition zone is the most effective

120   location for head and salinity simulations and observations. The sensitivity results in this study confirm some conclusions in Shoemaker (2004), and highlight the significance of conduit network on seawater intrusion in a coastal karst aquifer with interaction of a karst conduit and a porous medium.

        This study aims to understand the impact factors of seawater intrusion to a coastal

125   karst aquifer, and provides guidelines for freshwater resources management. The parameter sensitivities are evaluated to address the effects of the two major challenges in this study, the density-dependent processes and the dual-permeability aquifer system in the model. To our knowledge, this is the first attempt to assess the parameter sensitivities for seawater intrusion to a vulnerable dual-permeability karst aquifer with a conduit

130   network. The rest of the paper is arranged as follows: the details of local and global sensitivity analysis are introduced in Sect. 2. The model setup, hydrological conditions, model discretization, initial and boundary conditions are discussed in Sect. 3. The results

of local and global sensitivity analysis are discussed in Sect. 4. The scenarios of seawater intrusion simulation with different boundary conditions and elapsed time are presented in

135   Sect. 5. The conclusions are made in Sect. 6.

2. Methods

The governing equations used in the SEAWAT model can be found in the Guo and Langevin (2002), including the variable-density flow equation with additional

140   density terms, and the advection dispersion solute transport equation. The local and global sensitivity methods used in this study are briefly introduced below. Note that the sensitivity analysis does not necessarily need field observations, but only evaluates the model simulations with respect to parameters instead. Field observational data, especially the head and salinity measurements within the conduit, are usually not available. Model

145   calibration is beyond the scope of this study, due to the lack of observational data in the WKP.

2.1 Local sensitivity analysis

In this study, UCODE_2005 (Poeter and Hill, 1998) is used in the local sensitivity

150   analysis, which evaluates the derivatives of model simulations with respect to parameters at the specified values (Hill and Tiedeman, 2006). The forward difference approximation of sensitivity is calculated as the derivative of the ith simulation respect to the jth model parameters,

$$\left.\frac{\partial y'_i}{\partial x_j}\right|_b \approx \frac{y'_i(x + \Delta x) - y'_i(x)}{\Delta x_j} \qquad 1)$$

where y'_i is the value of the ith simulation; x_j is the jth estimated parameter; x is a vector of the specified values of estimated parameter; Δx is a vector of zeros except that the jth parameter equals Δx_j.

The sensitivities are calculated by running the model once using the parameter values in x to obtain $y'_i(x)$, and then changing the jth parameter value and running the model again in $x + \Delta x$ to obtain $y'_i(x + \Delta x)$. Scaled sensitivities are used to compare the parameters sensitivities that may have different units. In UCODE_2005, a scaling method is used to calculate the dimensionless scaled sensitivities (DSS) by the following equation,

$$dss_{ij} = \left(\frac{\partial y'_i}{\partial x_j}\right)\bigg|_x |x_j| \omega_{ii}^{1/2} \qquad 2)$$

where dss_{ij} is the dimensionless scaled sensitivity of the ith simulation with respect to the jth parameter; ω_{ii} is the weight of the ith simulation.

The DSS values of different simulations with respect to each parameter are accumulated as the composite scaled sensitivities (CSS). The CSS of the jth parameter is evaluated via:

$$css_j = \sum_{i=1}^{ND}\left[(dss_{ij})^2\big|_x / ND\right]^{1/2} \qquad 3)$$

where *ND* is the number of simulated quantities, for example, the head and salinity simulations in this study.

2.2 Morris method for global sensitivity analysis

The local sensitivity analysis is conceptually straightforward and easy to compute without expensive computational cost. However, it calculates only at one specified value

for each parameter instead of the entire parameter ranges. In addition, the indices are approximated in the first order derivative only, assuming a linear relationship of

175 simulated quantities with respect to parameters.

The global sensitivity analysis evaluates the parameters which may be considered to have the non-linear effects with simulations, and/or involved in interaction with other factors. Morris method is applied to evaluate the global parameter sensitivities in this study (Morris, 1991). The experimental plan proposed by Morris is composed of

180 individually randomized "one-step-at-a-time" (OAT) experiment, which perturbs only one input parameter and gives a new value in each run. The Morris method is made by a number r of local changes at different points of the possible range of input values. In each parameter, a discrete number of values called levels are chosen with the parameter ranges of variation.

185 In Morris method, the k-dimensional vector x of the model parameters has components x_i to be divided into p uniform intervals. The global sensitivity is evaluated by the simulation results with changing one parameter at a time, which is called an elementary effect (*EE*), d_i, defined as,

$$d_i = \frac{1}{\tau_y} \frac{[y(x_1{}^*, \dots, x_{i-1}{}^*, x_i{}^* + \Delta, x_{i+1}{}^*, \dots, x_k{}^*) - y(x_1{}^*, \dots, x_k{}^*)]}{\Delta} \qquad 4)$$

where Δ is the relative distance in the coordinate; τ_y is the output scaling factor; $\{x_i{}^*\}$ is

190 the parameter set selected in a sampling method.

To compute the EE for the k parameters, $(k+1)$ simulations will run with perturbation of each parameter, which is called one "path" (Saltelli et al., 2004). An

ensemble of EEs for each parameter is generated by multiple paths of parameter set. The total number of calculation is $r(k+1)$, where r is the number of paths.

195   Two sensitivity measures are proposed by Morris method for each parameter: the mean μ estimates the overall influence of the factor on the output, and the standard deviation σ estimates the non-linear effect between input and output, and/or the parameter interactions (Saltelli et al., 2004). The mean μ and standard deviation σ of the EEs are evaluated with the r independent paths in the Morris method,

$$\mu = \sum_{i=1}^{r} d_i/r \qquad \text{5)}$$

$$\sigma = \sqrt{\sum_{i=1}^{r}(d_i - \mu)^2/r} \qquad \text{6)}$$

200

In this study, the EEs for the method of Morris are not generated by Monte Carlo random sampling, which usually needs extremely large numbers (>250) of paths for 11 parameters and takes a very long time to complete sensitivity computation without parallelization. To save the running time and computational cost but ensure the reliability

205   of sensitivity results, the more efficient trajectory sampling is developed by Saltelli et al. (2004) and becomes a widely-used method to generate the ensembles of EEs for Morris method. In trajectory method, the choice of parameter p and Δ of the design is p even and $\Delta = \pm p/[2(p-1)]$, either positive or negative. The trajectory method starts by randomly selecting a "base" value x^* for the vector x. Each component x_i of x^* is sampled from the

210   set $(0, 1/(p\text{-}1), 2/(p\text{-}1), \dots ,1)$. The randomly selected vector x^* is used to generate the

other sampling points but not one of them, which means that the model is never evaluated

at vector x^*. The first sampling point, $x^{(1)}$, is obtained by changing one or more

components of x^* by Δ. The choice of components x^* to be increased or decreased is

conditioned on that $x^{(1)}$ still being within the domain. The second sampling point, $x^{(2)}$, is

215   generated from x^* but differs from $x^{(1)}$ in its ith component that has been either

increased or decreased by Δ, but conditioned on the domain, and the index i is randomly

selected in the set $\{1,2, ..., k\}$. In other word, $x^{(2)} = (x_1^{(1)}, ..., x_{i-1}^{(1)}, x_i^{(1)} \pm$

$\Delta, x_{i+1}^{(1)}, ..., x_k^{(1)})$. The third sampling point, $x^{(3)}$, differs from $x^{(2)}$ for only one component

j, for any $j \neq i$, will be $x_j^{(3)} = x_j^{(2)} \pm \Delta$. A succession of $(k+1)$ sampling points

220     $x^{(1)}, x^{(2)}, ..., x^{(k+1)}$ is produced in the input parameters space called a trajectory, with the

key characteristic that two consecutive points differ in only one component. In the

trajectory sampling, any component i of the "base" vector x^* has been selected at least

once by Δ in order to calculate one EE for each parameter.

     Once a trajectory has been constructed and evaluated by Morris method, an EE

225   for each parameter i, $i = 1, ..., k$, can be computed. If $x^{(l)}$ and $x^{(l+1)}$, with l in the set in

$(1, ..., k)$, are two sampling points differing in their ith component, the EEs associated

with the parameter i is computed as,

$$d_i\left(x^{(l)}\right) = \frac{[y(x^{(l+1)}) - y(x^{(l)})]}{\Delta}, \qquad\qquad 7)$$

     A random sample of r EEs is selected at the beginning of sampling, and the

starting point of each trajectory sampling is also randomly generated. The points

230   belonging to the same trajectory are not independent, but the r points sampled from each

distribution belonging to different trajectories are independent.

3. Model development

3.1 Study site

235   The numerical model developed in this paper studies the real dimension and parameter values of a porous medium and a conduit in the aquifer at the Woodville Karst Plain (WKP). The Spring Creek Springs (SCS) is a first magnitude spring in the WKP, consisting of 14 submarine springs located in the Gulf of Mexico (Fig. 1). SCS is an outlet of the subsurface conduit network and the entrance of seawater intrusion, exactly

240 located at the shoreline beneath the sea level. Davis and Verdi (2014) developed a groundwater cycling conceptual model to explain the hydrogeological conditions in the WKP. They introduced that seawater intrudes through subsurface conduit networks during low precipitation periods, while rainfall recharge pushes the intruded seawater out of the aquifer after a heavy storm event. Later on, this conceptual model of the seawater

245 and freshwater interactions in the WKP is quantitatively simulated by a constant-density CFPv2 numerical model (Xu et al., 2015b). In this study, the seawater intrusion process via the SCS through the conduit network is simulated by the density-dependent 2D SEAWAT model. Tracer test studies and cave diving investigations indicate that the conduit system starts from the submarine spring and extends 18 km landward connecting

250 with an inland spring called Wakulla Spring, although the exact locations of the subsurface conduits are unknown and difficult to explore (Kernagis et al., 2008; Kincaid and Werner, 2008). Evidence shows that seawater intrusion has been observed through subsurface conduit system for more than 18 km in the WKP (Xu et al., 2016). In addition, Davis and Verdi (2014) also point out that sea level rise at the Gulf of Mexico in the past

255   century could be a reason for increasing discharge at an inland karst spring (Wakulla

Spring) and decreasing discharge at SCS, when the hydraulic gradient between the two

springs is directed towards the Gulf.

(Insert Fig. 1 here)

In this study, a two-dimensional SEAWAT model is set up to simulate seawater

260   intrusion through the major subsurface conduit network in the WKP (Fig. 1). Figure 2

presents the cross section schematic figure in a coastal karst aquifer with a conduit

network and a submarine spring opening to the sea. The model spatial domain is not a

straight line from the SCS to Wakulla Spring, but the cross section along the major

conduit pathway of seawater intrusion between the two springs. The conduit geometry in

265   the model is set as 18-km long and 91-meter deep with a diameter of 10 meters

horizontally and 50 meters vertically.

(Insert Fig. 2 here)

Since the main purpose of this study is to evaluate the effects of subsurface

conduit parameters on modeling seawater intrusion in the coastal karst aquiferseawater

270   intrusion through the conduit network, salinity plume in the porous medium and the

exchanges between the two systems are simulated only within the vertical cross section.

The simulation of saltwater intrusion within the horizontal plane is beyond the scope of

the two-dimensional SEAWAT model in this study. The assumption of two-dimensional

model is reasonable and sufficient for understanding the parameter sensitivities, since the

275   horizontal exchange flux between the conduit and the surrounding porous medium is

trivial, when the exchange permeability on the conduit wall is much smaller than the

large conduit hydraulic conductivity. In addition, most SEAWAT models are setup for

two-dimensional cross section with high-resolution vertical discretization. Three-dimensional density-dependent flow and transport model is rarely seen and applied, due

280   to the computational constraint.

3.2 Hydrological parameters

Table 1 presents the hydrological parameter values of the Upper Floridan Aquifer (UFA) in the WKP and boundary conditions used in the model. These parameters have

285   been calibrated in the regional-scale groundwater flow and solute transport models by Davis et al. (2010), and then been applied in many previous modeling studies (Gallegos et al., 2013; Xu et al., 2015a; Xu et al., 2015b). It should be pointed out that this study does not aim to re-calibrate the model, since the observational field data are insufficient. The head and salinity measurements in the conduit are rarely available, considering the

290   difficulties of monitoring devices installation in the subsurface conduit. The parameter values are evaluated in the following local sensitivity analysis and applied in the seawater intrusion scenarios in Sect. 5.

(Insert Table 1 here)

The values of hydrological parameters (hydraulic conductivity, specific storage

295   and effective porosity) in the conduit are generally greater than those surrounding porous medium. Hydraulic conductivity of the porous medium is assigned as 2286 m/day (7500 ft/day), and as large as 610,000 m/day (2,000,000 ft/day) for the conduit system. Even the hydraulic conductivity of porous medium in the study region is larger than most alluvial aquifers, because numerous small fractures and relatively large pores existed in the karst

300   aquifer due to dissolution of carbonate rocks. Specific storage and effective porosity in

the porous medium are assumed as 5×10^{-7} and 0.003, respectively. Specific storage and

effective porosity are 0.005 and 0.300 in the conduit layer, respectively. The longitudinal

dispersivity is estimated as 10 m in the porous medium, but is assumed a very small value

(0.3 m) in the conduit, because advection is dominated and dispersion is negligible in the

305   solution of transport in the conduit.

3.3 Spatial and temporal discretization

        The grid discretization and boundary conditions of the two-dimensional

SEAWAT numerical model are shown in Fig. 3, with 140 columns and 37 layers in the

310   cross section. Guo and Langevin (2002); Werner et al. (2013) pointed out that refining

vertical grid resolution is required for accurately modeling the density-dependent flow

and solute transport. The vertical thickness of each grid cell is set uniformly as 3.048 m

(10 ft) in this study, significantly smaller than the 152 m (500 ft) thickness in many

previous constant-density modeling studies in the WKP, for example, Davis and Katz

315   (2007); Davis et al. (2010); Xu et al. (2015a); Gallegos et al. (2013); Xu et al. (2015b).

(Insert Fig. 3 here)

        The horizontal discretization for each cell is set uniformly as 152 m (500 ft) as the

scales in the field, except columns #22 and #139, which are 15.2 m (50 ft) as the vertical

conduit network connecting the submarine spring (SCS) and inland spring (Wakulla

320   Spring), respectively. The sizes of spring outlets and the conduit are based on the

observational field data and the calibrated values from the previous studies (Gallegos et

al., 2013). However, the diameter of horizontal conduit network is assumed constant in

this study. The outlet of vertical conduit system is the submarine spring (SCS) located at

the shoreline at column #22. The conduit system starts from the submarine spring,

325 descends downward to layer #29 (nearly 100 m below sea level), horizontally extends

nearly 18 km from column #22 to column #139, and then rises upward to the top through

column #139. Seawater intrudes at the SCS on the first layer of column #22, and then

flows vertically downward into the conduit system. The inland spring is simulated by the

DRAIN package as general head boundary condition in the SEAWAT model. All layers

330 are simulated as confined aquifer since the conduit is fully saturated, which are consistent

to the previous numerical models used in Davis et al. (2010); Xu et al. (2015a); Xu et al.

(2015b) in the WKP.

   A transient 7-day stress in the SEAWAT model is evaluated throughout this

study. The scenarios of longer simulation time are exceptions for evaluating seawater

335 intrusion under an extended low rainfall period in Sect. 5.4. The timestep of flow model

is set as 0.1 days, and the timestep of transport model is determined by SEAWAT

automatically.

3.4 Initial and boundary conditions

340   The initial condition of head is constant within each layer, set as 0.0 m as the

present-day sea level for the cells from the boundary on the left (column #1) to the

shoreline (column #22), and gradually rises to 1.52 m (5.0 ft) at inland boundary on the

right, determined by the elevation of Wakulla Spring. Note that the head values are

written in the input files of SEAWAT model instead of equivalent freshwater head. The

345 initial conditions of salinity are assumed as a constant value of 35.0 PSU (Practical

Salinity Unit) with each layer as seawater without mixing at the sea boundary and the

leftmost 10 columns. The seawater/freshwater mixing zone is assumed from 35 PSU at

column #11 to 0 PSU at column #45, with a gradient of 1.0 PSU per column. Salinity is

set uniformly as 0.0 PSU from column #46 to the inland boundary on the right, as

350   uncontaminated freshwater before seawater intrudes. Several testing cases have been

made to confirm that the initial conditions trivially affect the modeling results.

The boundary conditions are also presented in Fig. 3. The less-permeable

confining unit of the UFA base is simulated at the bottom of model domain as no-flow

boundary condition. The constant head and concentration inland boundary condition on

355   the right is 1.5 m (5.0 ft) as the elevation of inland spring, and 0.0 PSU as

uncontaminated freshwater. The seawater boundary on the left is 3.38 km away from the

shoreline, set as 0.0 m constant head as the present-day sea level and 35.0 PSU constant

concentration as seawater without mixing. The boundary conditions of head and salinity

at the submarine spring (column #22, layer #1) are adjusted and evaluated in the

360   scenarios of different sea level, salinity and rainfall conditions in Sect. 5.

4. Sensitivity Analysis

Sensitivity analysis evaluates the uncertainties of salinity and head simulations

with respect to eleven parameters, helps to understand the effects of variations of aquifer

365   parameters and boundary conditions on simulation. The symbols and definitions of the

eleven parameters are listed in Table 1, as well as the values computed in the local

sensitivity analysis, and the parameter ranges evaluated in the global sensitivity analysis

(Table 1). There are six parameters in the groundwater flow model, including hydraulic

conductivity (HY_P and HY_C), specific storage (SS_P and SS_C) of the conduit and the

370   porous medium, recharge rate (RCH) and the sea level at the submarine spring (H_SL).

The other five parameters, including effective porosity (PO_P and PO_C), dispersivity

(DISP_P and DISP_C) of the conduit and the porous medium, and the salinity at the

submarine spring (SC), are in the solute transport model.

375   **4.1 Local sensitivity analysis**

In the local sensitivity analysis, the CSSs (composited scaled sensitivities) of

parameters with respect to head and salinity simulations are calculated along the conduit

network and within the porous medium. The CSSs are computed for the parameter values

of the maximum seawater intrusion benchmark case in Sect. 5.1, which is developed to

380   quantitatively evaluate the extent of seawater intrusion in a coastal karst aquifer,

specifically with the hydrological parameters in the WKP. The local sensitivity analysis

is also used to determine the parameters to be adjusted and evaluated in the scenarios.

Parameter sensitivities are computed at several locations, from column #25 to

column #75 with an interval of 5 cells along the horizontal conduit (layer #29), where

385   column #25 is the near shore aquifer fully contaminated by seawater, and column #75 is

assumed as the uncontaminated freshwater aquifer. The parameter sensitivities of

simulations in a porous medium are evaluated at layer #24, 15.2 m (50 ft) or 5 layers

above the conduit layer, from column #25 to column #75 with an interval of 5 cells along

the horizontal direction.

390

4.1.1 Local sensitivity analysis of simulations in the conduit

Figure 4 shows the arithmetic mean of CSSs computed in the evaluated locations along the conduit layer. The largest CSS value indicates that salinity at the submarine spring (SC) is the most important parameter to both salinity and head simulations. Hydraulic conductivity, specific storage and effective porosity of the conduit (HY_C, SS_C and PO_C), as well as the sea level at the submarine spring (H_SL) are also important parameters. Simulations are not sensitive to hydraulic conductivity, specific storage and effective porosity of the porous medium (HY_P, SS_P and PO_P), recharge rate (RCH) and dispersivity (DISP_C and DISP_P). Generally speaking, the parameter sensitivities with respect to head simulations are similar and consistent with salinity simulations.

(Insert Fig. 4 here)

The boundary conditions of the conduit system, including salinity and sea level at the submarine spring (SC and H_SL), are important in modeling seawater intrusion in the WKP. Seawater enters the conduit system at the submarine spring, and intrudes landward through the subsurface conduit system. The most important parameter is identified as the salinity at the submarine spring (SC), which determines the equivalent freshwater head in terms of water density at the inlet of conduit system, and affects flow simulation within the conduit system as well as the surrounding porous medium via exchange on the conduit wall. The salinity at the submarine spring (SC) is determined by freshwater mixing and dilution from the conduit network, in other words, is controlled by the rainfall recharges and freshwater discharge from the aquifer to the sea. In this study, rainfall recharge is represented by salinity at submarine spring with freshwater dilution. Recharge

flux on the surface (RCH) is not an important parameter, and is not applicable to

415   represent the total rainfall recharge in a two-dimensional SEAWAT model. On the other

hand, the sea level at the submarine spring (H_SL) also has an intermediate CSS rule on

flow field and salinity transport simulations. However, it is not as important as the

salinity at the submarine spring (SC). In other words, the extent of seawater intrusion in

the conduit is more sensitive to rainfall recharge and freshwater discharge represented by

420   the parameter SC, rather than the sea level and/or tide level variations.

Dispersivity is usually an important parameter in the sensitivity analysis of

transport modeling in a porous medium aquifer. However, the conduit and porous

medium dispersivities (DISP_C and DISP_P) are not important parameters for salinity

and head simulations in this study. Advection is dominated in the transport of seawater

425   within the highly permeable conduit network, while dispersion is negligible in such high-

speed flow condition. Meanwhile, the dispersion solution and dispersivity sensitivities in

the conduit are inaccurately calculated when conduit flow becomes turbulent. On the

other hand, the numerical dispersion is significantly greater than the solution of physical

dispersion in the conduit. The Peclet number can be as great as 2500, far beyond the

430   theoretical criteria (<4) for solving the advection dispersion transport equation by finite

difference method. The dispersivity sensitivities are computed with large uncertainty,

indicating that the continuum SEAWAT model is not applicable to accurately compute

the salinity dispersion in the conduit.

The parameters with the six largest CSS are presented in Fig. 5, with respect to

435   the combination of head and salinity simulations in the evaluated locations along the

conduit network, from column #25 to column #75. The largest CSS values are found at

either column #50 or #55 within the conduit, matches the position of seawater/freshwater

mixing zone along the conduit network in the maximum seawater intrusion case (Sect.

5.1). All parameters have the CSS values at the mixing zone than anywhere else, because

440   head and salinity simulations only change significantly near the mixing zone but remain

constant in other locations.

(Insert Fig. 5 here)

4.1.2 Local sensitivity analysis of simulations in the porous medium

445   Figure 6 shows the arithmetic mean of CSSs computed in the evaluated locations

in the porous medium (layer #24). The largest CSS value indicates that salinity at the

submarine spring (SC) is also the most important parameter with respect to simulations in

the porous medium, although it is a boundary condition of the conduit system. However,

some parameter sensitivities are different from the results of simulations in the conduit.

450   The hydraulic conductivity and effective porosity of both the conduit and porous medium

(HY_C, HY_P, PO_C & PO_P), specific storage of the conduit (SS_C) and dispersivity

of the porous medium (DISP_P), have intermediate CSS values. The CSS values at

different evaluated locations along the layer of porous medium are plot in Fig. 7, except

the three unimportant parameters. Similar to the sensitivity analysis of simulations along

455   the conduit, the largest CSSs are found at either column #35 or #40, which is the mixing

zone position in the porous medium in the maximum seawater intrusion case (Sect. 5.1).

(Insert Fig. 6 and 7 here)

        The important rules of the boundary condition and hydrological parameters of the

conduit system on simulations in the porous medium are highlighted in the local

460   sensitivity analysis. Salinity at the submarine spring (SC) remains the most important

parameter and determines the seawater intrusion plume in the porous medium. The

conduit hydrological parameters, such as hydraulic conductivity, effective porosity and

specific storage (HY_C, PO_C and SS_C), are also important for the simulations in the

porous medium. The CSSs of conduit parameters indicate that groundwater flow and

465   seawater transport through the conduit system have significant impact on the head and

salinity simulations in the surrounding porous medium. In summary, simulations in the

porous medium are sensitive to the hydrological parameters of both the conduit and the

porous medium, indicating that the interaction between the two domains are important for

simulating seawater intrusion in the dual-permeability WKP coastal karst aquifer. As a

470   result, simulations and observations of salinity and head in the conduits and other karst

features have significance on calibrating numerical models and values for understanding

seawater intrusion in the WKP.

4.2 Global sensitivity analysis

475   The local sensitivity analysis is conducted to analyze the parameter sensitivities

specifically for the seawater intrusion in the WKP after a 7-day low precipitation period,

as the maximum seawater intrusion cases in Sect. 5.1. However, local sensitivity result is

lack of representative for the entire parameter ranges, higher-order derivatives. The

global sensitivity analysis is necessary to evaluate a comprehensive relationship between

480   simulations and parameters for modeling seawater intrusion to a coastal karst aquifer.

Figure 8 presents the derivatives of simulations with respect to the selected

parameters in order to evaluate if the CSS values in the local sensitivity analysis is

representative within the entire parameter range. For example, head and salinity simulations in the conduit are nearly constant to the variation of the unimportant

485   parameter (DISP_P) in the local sensitivity study. Simulations in the porous medium are linear to parameter HY_P with an intermediate value. However, both head and salinity simulations are non-linear to salinity at the submarine spring (SC), which is the most important parameter identified in the local sensitivity analysis (Fig. 8). The CSS value of parameter SC is computed at the largest derivative value where salinity is 35 PSU.

490   (Insert Fig. 8 here)

The locations in the conduit and porous medium systems with the largest CSS values from the local sensitivity analysis are evaluated in the global sensitivity analysis. Parameter sensitivities are computed at the specified location in the conduit (column #50, layer 29) and the porous medium (column #35, layer #24), respectively. The Trajectory

495   sampling method developed by Saltelli et al. (2004) is introduced in Sect. 2.2 and applied in this study, with the recommended choice of $p = 4$ and $r = 10$ by Saltelli et al. (2004).

4.2.1 Global sensitivity analysis of simulations in the conduit

In the global sensitivity analysis, the mean and standard deviation of the EEs for

500   salinity simulation in the conduit (column #50, layer #29) are presented in Fig. 9a. The largest EE mean value indicates that parameter SC is the most important parameter to salinity simulations. It is consistent with the local sensitivity result, since the submarine spring is the boundary condition of the major pathway for seawater intrusion to the aquifer. The largest standard deviation of the EEs is due to the non-linear relationship

505   between salinity simulation and parameter SC shown in Fig. 8, in which the derivatives

vary with different parameter values. The hydraulic conductivity and effective porosity of

the conduit (HY_C and PO_C), as well as sea level (H_SL), are all important to salinity

simulation with relatively large mean and standard deviation values of EEs. Generally

speaking, the global sensitivity study results for salinity simulation in the conduit are

510   similar to the local sensitivity results.

(Insert Fig. 9 here)

The global sensitivities of head simulations with respect to parameters are more

complicated than salinity simulations (Fig. 9b). The mean and standard deviation of EEs

for head simulations are smaller than those for salinity simulations, consistent with the

515   conclusion that salinity simulation is more effective than head (Shoemaker, 2004).

Different from salinity simulation, salinity at the submarine spring (SC) no longer has the

largest mean but standard deviation, due to the non-linear relationship to head simulation

shown in Fig. 8. Head simulations are also sensitive to the boundary conditions of salinity

in the transport model when salinity is high, because equivalent freshwater head is a

520   function of density in terms of salinity in the coupled variable-density flow and transport

model for simulating seawater intrusion.

In this study, parameters in transport model are also important to the head

simulation in a coupled density-dependent flow and transport model. The two largest

mean values of EEs show that the specific storage (SS_C) and effective porosity (PO_C)

525   of the conduit are the two most important parameters. Specific storage and effective

porosity are parameters in the coupled density-dependent flow and transport model,

respectively, determined by the void space in the aquifer from field measurement. Head

simulation is usually not a function of effective porosity when transport equation is

solved separately after the flow model is computed in the constant-density simulation.

530   Effective porosity is important in head simulation since the solution of salinity transport in turn determines the density and impact flow calculation in the model, particularly in the study of density-dependent seawater intrusion. This is also consistent with the previous sensitivity study using the SEAWAT model (Shoemaker, 2004).

The other major finding in the global sensitivity analysis is that the hydraulic

535   conductivity of the conduit (HY_C) is no longer the most important parameter, with smaller means and standard deviations of EEs than the other two parameters (PO_C and SS_C). The sensitivity result is different from the common knowledge and empirical experience in hydrogeological modeling, but is actually reasonable in karst aquifer with the non-laminar conduit flow. In the SEAWAT model, Darcy equation is used to

540   calculate the flow velocity in the whole model domain including the conduit system, however, is only accurate for laminar seepage flow in the porous medium. Groundwater flow easily becomes non-laminar even turbulent in the giant conduit system, when the conduit flow discharge is non-linear to head gradient and hydraulic conductivity. The simulation of conduit flow is beyond the applicability of Darcy equation in SEAWAT

545   model, with relatively large error and uncertainty in the relationship between hydraulic conductivity and head simulation.

4.2.2 Global sensitivity analysis of simulations in the porous medium

The global sensitivity analysis has different results for some non-linear parameter

550   sensitivities, highlights the interaction between the conduit and porous medium systems. Parameters HY_P and SC are identified as the two most important parameters for salinity

simulations in the porous medium (Fig. 10a). Compared with hydraulic conductivity of the porous medium (HY_P) ,the parameter SC has much larger CSS value in the local sensitivity analysis (Fig. 6), and also larger mean of EE in the global sensitivity analysis.

555 Simulations are non-linear to the parameter SC, which is evaluated at 35.0 PSU with the largest derivative in the local sensitivity analysis (Fig. 8). In other words, local sensitivity analysis overestimates the sensitivity of parameter SC within the range, and global sensitivity analysis provides a more comprehensive understanding of the variability of rainfall recharges and freshwater discharge. As the boundary condition of conduit system,

560 salinity at the submarine spring (SC) determines the equivalent freshwater head at the inlet of seawater intrusion and affects simulations in the conduit, and also the surrounding porous medium via exchanges between the two systems. Similar to the largest CSS value of parameter SC in the local sensitivity result, the global sensitivity result highlights the significance of the interaction between the conduit and the porous medium domains in a

565 dual-permeability aquifer. Similar to salinity at the submarine spring (SC), the relatively large mean of EEs for sea level (H_SL), effective porosity and specific storage of the conduit (PO_C and SS_C) highlight the values of dynamic interaction between the conduit and the porous medium in this study.

(Insert Fig. 10 here)

570 On the other hand, parameter sensitivities for simulations in the porous medium exhibit different characteristics from those in the conduit. The porous medium hydraulic conductivity (HY_P) is an important term in the flow equation for solving head and advective velocity for the transport equation (Fig. 10b), similar to most sensitivity result of hydrological modeling for flow in a porous medium. Please note this is different from

575   the global sensitivity results of simulations in the conduit, in which the EEs of effective

porosity and specific storage of the conduit (PO_C and SS_C) have larger mean and

standard deviation values than hydraulic conductivity (HY_C), because of the uncertainty

of conduit flow calculation by Darcy's equation in the continuum SEAWAT model. As

the boundary condition of the conduit, parameter H_SL affects head solutions in the

580   surrounding porous medium by determining the head-dependent exchange flux between

the two domains. Generally, the impacts of boundary conditions (SC and H_SL) and

hydrological properties (SS_C, HY_C and PO_C) of the conduit system on head

simulations in the porous medium are significant and important. In addition, effective

porosity of the porous medium (PO_P) also has relatively large mean and standard

585   deviation of EEs for head simulations, since the density-dependent flow and transport

models are coupled for simulating seawater intrusion.

Dispersivity is no longer an important parameter in such a dual-permeability

aquifer, conflicted with Shoemaker's (2004) result that dispersivity is an important

parameter in a homogeneous porous medium domain without the preferential advective

590   flow. In a dual-permeability karst aquifer system, advection transport is dominated in the

conduit and the surrounding porous medium as well, while dispersion becomes

unimportant. In this study, the uncertainty of dispersivity sensitivities can be significant

when the Peclet number in the conduit is large beyond its criteria for solving transport

equation by finite difference method, which requires the Peclet number to be smaller than

595   4. An experiment of deactivating the DSP (dispersion) package in SEAWAT confirms

that dispersion is negligible within the conduit network in this study, and the mixing is

mostly due to the numerical dispersion instead of the solution of dispersion equation in this study.

600 **5. Seawater Intrusions Scenarios**

In this section, the the extents of seawater intrusion are quantitatively measured and evaluated under scenarios of boundary conditions, which are identified as the important parameters in the local sensitivity analysis. In each scenario, only one parameter is adjusted and others remain the same as the original values in the maximum

605 seawater intrusion benchmark case.

5.1 The maximum seawater intrusion benchmark case

The head and salinity boundary conditions are set as 0.0 m as the present-day sea level, and 35.0 PSU as seawater without dilution at the conduit system outlet,

610 respectively. The local sensitivity analysis computes the sensitivities of parameter values in the maximum seawater intrusion benchmark case . Salinity and sea level at the submarine spring (SC and H_SL) are identified as two important parameters and then adjusted in the following two scenarios. In this case, the longest distance of seawater intrusion is simulated by assuming that freshwater recharge is negligible, and the outlet of

615 conduit system is filled with undiluted seawater. Figure 11 presents the simulated salinity and head profile in the cross section after a 7-day simulation.

 (Insert Fig. 11 here)

According to the Ghyben-Herzberg relationship, high-density seawater intrudes landward through the bottom of the aquifer beneath the freshwater flowing seaward on

620   the top. The equivalent freshwater head at the submarine spring is calculated as 2.29 m (7.5 ft) when salinity is 35.0 PSU at the submarine spring, and undiluted seawater is filled within the 91 meters deep submarine cave connecting to the conduit. The equivalent freshwater head at the submarine spring is higher than the 1.52 m (5.0 ft) constant head at the inland spring, diverts the hydraulic gradient landward and causes seawater to intrude

625   into the aquifer. Seawater intrudes further landward through the highly permeable conduit network, also contaminates the surrounding porous medium via exchange on the conduit wall. The seawater/freshwater mixing zone in the deep porous medium beneath the conduit is only slightly behind the seawater front in the conduit, because high-density saline water easily descends from the conduit. The area with relatively smaller salinity to

630   the left of the vertical conduit network near shore is due to the freshwater discharge dilution from the aquifer to the sea, since the equivalent freshwater head is only set as 2.29 m at the submarine spring but remains as 0 m in other areas. The simulated salinity profile shows that the mixing zone position in the conduit, defined as the location with salinity of 5.0 PSU, is nearly 5.80 km landward from the shoreline. The width of mixing

635   interface, defined as the distance between the locations with salinity of 1.0 PSU and 25.0 PSU, is about 7 grid cells or 1.13 km (0.7 miles) and roughly the same in both the conduit and porous medium.

5.2 Salinity variation at the submarine spring (SC)

640   Sensitivity analysis indicates that the salinity at the submarine spring (SC), controlled by the rainfall dilution and regional freshwater recharge, is generally the most important parameter for simulations in both the conduit and the porous medium. Salinity

at the submarine spring is diluted by large amount of rainfall recharge and freshwater discharge after a significant precipitation event, but remains high after an extended low rainfall period, as shown in the maximum seawater intrusion benchmark case in Sect. 5.1. The equivalent freshwater head at the submarine spring is 2.29 m (7.5 ft) when salinity is 35.0 PSU, proportionally decreases to 0.0 m, where salinity is 0.0 PSU and freshwater is filled within the conduit system. The impact of freshwater recharge on seawater intrusion is evaluated in four scenarios with different salinity of 0.0 PSU, 10.0 PSU, 20.0 PSU and 30.0 PSU at the submarine spring (Fig. 12). The mixing zone in both the conduit and porous medium are located at 4.0 (4.5) km away from the shoreline in the cases of salinity of 10.0 (20.0) PSU at the submarine spring. Compared to the maximum seawater intrusion benchmark case, rainfall recharge and freshwater discharge move the interface significantly seaward. The mixing zone is very close to the shoreline when salinity is 0.0 PSU at the submarine spring and seawater intrusion is blocked by large amount of freshwater dilution. The shape of mixing interface is similar to the maximum seawater intrusion benchmark, but the width is significantly wider due to the smaller or even reversed hydraulic gradient from the aquifer to the sea. In the scenarios of freshwater dilution, the solution of dispersion becomes more accurate and important in salinity transport with slower groundwater seepage flow. Generally speaking, seawater no longer intrudes significantly inland after a heavy rainfall event, and the mixing interface moves seaward when freshwater dilutes the salinity within the conduit and the submarine spring. (Insert Fig. 12 here)

5.3 Sea level variation at the submarine spring (H_SL)

In addition to salinity, sensitivity analysis indicates that sea level at the submarine spring is also an important parameter. IPCC (2007) predicted an approximation of 1.0 m sea level rise at the beginning of next century, which has significant impacts on seawater intrusion in a coastal karst aquifer. The extents of seawater intrusion in the conduit and porous medium under 0.91 m (3.0 ft) and 1.82 m (6.0 ft) sea level rise conditions are quantitatively evaluated in this study (Fig. 13). Salinity at the submarine spring remains 35.0 PSU as the maximum seawater intrusion benchmark, but the head at the submarine spring increases as rising sea level. The simulated salinity profiles show that the width and shape of the mixing zone are similar to the simulated result in the maximum seawater intrusion benchmark. However, the mixing zone is pushed landward along the conduit to almost 7.08 km from the shoreline with 0.91 m (3.0 ft) sea level rises, which is 1.28 km further inland than the simulation with the present-day sea level. In the other extreme case of 1.82 m (6.0 ft) sea level rise, seawater intrudes additional 0.97 km further inland along the conduit than the simulated result of 0.91 m (3.0 ft) sea level rise, or 2.25 km further inland than the simulation with present-day sea level. Compared with the usual alluvial aquifer of porous medium, seawater intrudes further landward through the conduit network in the a dual-permeability karst aquifer under sea level rise. This scenario confirms the concerns of severe seawater intrusion in the coastal karst aquifer under sea level rise, also highlights the values of conduit system as the major pathway for long-distance seawater intrusion. In addition, sea level rise possibly have great impacts on the regional flow field and hydrological conditions in a coastal aquifer. Davis and Verdi (2014) reported an increasing groundwater discharge at the inland Wakulla Spring

in the WKP associated with the rising sea level in the past decades. The relationship

between spring discharge and sea level was quantitatively simulated by a CFPv2

690   numerical model in Xu et al. (2015b). However, the changes of flow field and

hydrological conditions are beyond the scope of this study.

(Insert Fig. 13 here)

5.4 Extended low rainfall period

695   The elapsed time in simulations are set constant in the sensitivity analysis and the

previous scenarios for consistent comparison purposes. However, extents of seawater

intrusion under scenarios of extended low rainfall periods are presented in Fig. 14, with

the extended simulated time of 14, 21 and 28 days. The boundary conditions of salinity

and sea level at the submarine spring remain 35.0 PSU and 0.0 m, respectively, as the

700   maximum seawater intrusion benchmark.

(Insert Fig. 14 here)

        Seawater intrudes through both the conduit and the porous medium domains

persistently during the extended low rainfall period, since the 2.29 m (7.5 ft) equivalent

freshwater head at the submarine spring is constantly higher than the inland freshwater

705   boundary. Compared with the maximum seawater intrusion benchmark with a stress

period of 7-day elapsed time in simulation, the mixing zone position moves additional

1.29 km landward in the conduit and the surrounding porous medium in the 14-day

simulation. In the predictions of 21 (28)-day extended low rainfall period, the mixing

zone finally arrives at 7.56 (7.89) km from the shoreline. Above all, seawater intrudes

710   further inland through conduit network during an extended low rainfall period,

contaminates fresh groundwater resources in the aquifer and becomes an environmental issue in coastal regions.

6. Conclusion

715   In this study, a two-dimensional SEAWAT model is developed to study seawater intrusion in a dual-permeability coastal karst aquifer with a conduit network. Local and global sensitivity analysis are used to evaluate the parameter sensitivities then help understand the values and importance of karst features in seawater intrusion. Some major conclusions from sensitivity analysis are summarized here,

720   1) The global sensitivity analysis is necessary to accurately estimate the parameter sensitivities in wider ranges, mainly due to the non-linear relationship between simulations and parameters. The parameter interactions are also important in this study. In the coupled density-dependent flow and transport model, head simulations are sensitive to boundary conditions and parameters of transport

725   equation, since the solution of salinity in terms of density affects the equivalent freshwater head calculation.

    2) Salinity at the submarine spring (SC) is the overall most important parameter. The boundary conditions and hydrological parameters of the conduit system are important to not only the simulations in the conduit, but also the porous medium

730   via exchanges between the two systems. The submarine spring and conduit system are the major entrance and pathway, respectively, for seawater intrusion in the coastal karst aquifer. Sensitivity analysis indicates that the simulations in the conduit are especially important for understanding the hydrogeological processes

seawater intrusion in such a dual-permeability karst aquifer, and field

735   observational data within the conduit system are necessary for the model

calibration.

3) Different from the previous studies in Shoemaker (2004), dispersivity is no longer

an important parameter for simulations in the conduit. Advection is dominant but

dispersion is negligible in the solution of salinity transport with turbulent flow in

740   the conduit, and the relatively fast seepage flow in the surrounding porous

medium. The interaction between conduit and porous medium significantly

change the flow field and affect the applicability of transport model. In the

simulated salinity profile, the mixing is mostly due to numerical dispersion

instead of the solution of dispersion equation, since the Peclet number is

745   extremely large in the domain and beyond the criteria of solving transport

equation by finite difference method.

4) Hydraulic conductivity is no longer an important parameter for simulations in the

conduit. Conduit flow easily becomes non-laminar and beyond the capability of

Darcy equation in SEAWAT model, which assumes a linear relationship between

750   specific discharge and head gradient. Therefore, the uncertainty of conduit

permeability is difficult to be accurately evaluated by hydraulic conductivity in

the continuum model.

The extents of seawater intrusion and width of mixing interface are quantitatively

measured with the variations of salinity and sea level at the submarine spring, which are

755 identified as important parameters in the sensitivity study. In the maximum seawater

intrusion benchmark case with salinity and head as 35.0 PSU and 0.0 m at the submarine

spring, respectively, the mixing zone in the conduit moves to 5.80 km from the shoreline

with 1.13 km wide after a 7-day low rainfall period. Rainfall and regional recharges

dilute the salinity at the submarine spring (SC), and significantly shift the mixing zone

760   position seaward to 4.0 (4.5) km away from the shoreline with salinity of 10.0 (20.0) PSU.

Compared with the benchmark, seawater intrudes additional 1.29 (2.25) km further

landward along the conduit under 0.91 (1.82) m sea level rise at the submarine spring

(H_SL). In addition, the impacts of an extended low rainfall period on seawater intrusion

through conduit network are also quantitatively assessed with longer elapsed time in

765   simulation. The mixing zone moves to 7.56 (7.89) km from the shoreline, after a 21 (28)-

day low precipitation period.

In a summary, the modeling and field observations in the karst features, including

the subsurface conduit network, the submarine spring and karst windows, are critical for

understanding seawater intrusion in a coastal karst aquifer, and important for model

770   calibration. The discrete-continuum density-dependent flow and transport model is

necessary to accurately simulate seawater intrusion and assess parameter sensitivities in

the coastal karst aquifer with conduit networks. The advanced numerical methods are

expected to solve the issue of Peclet number limitation in this study and compute more

accurate solution of dispersion.

775

Competing interests

The authors declare that they have no conflict of interest.

References

780 Bear, J.: Seawater intrusion in coastal aquifers, Springer Science & Business Media, 1999.

Calvache, M., and Pulido-Bosch, A.: Effects of geology and human activity on the dynamics of salt-water intrusion in three coastal aquifers in southern Spain, Environmental Geology, 30, 215-223, 1997.

785 Custodio, E.: Salt-fresh water interrelationships under natural conditions, Groundwater Problems in Coastal Areas, UNESCO Studies and Reports in Hydrology, 45, 14-96, 1987.

Davis, J. H.: Hydraulic investigation and simulation of ground-water flow in the Upper Floridan aquifer of north central Florida and southwestern Georgia and delineation of

790 contributing areas for selected City of Tallahassee, Florida, Water-Supply Wells, U.S. Geological Survey, Tallahassee, Florida, 55, 1996.

Davis, J. H., and Katz, B. G.: Hydrogeologic investigation, water chemistry analysis, and model delineation of contributing areas for City of Tallahassee public-supply wells, Tallahassee, Florida, Geological Survey (US)2328-0328, 2007.

795 Davis, J. H., Katz, B. G., and Griffin, D. W.: Nitrate-N movement in groundwater from the land application of treated municipal wastewater and other sources in the Wakulla Springs Springshed, Leon and Wakulla counties, Florida, 1966–2018, US Geol Surv Sci Invest Rep, 5099, 90, 2010.

Davis, J. H., and Verdi, R.: Groundwater Flow Cycling Between a Submarine Spring and

800 an Inland Fresh Water Spring, Groundwater, 52, 705-716, 2014.

Diersch, H.: FEFLOW reference manual, Institute for Water Resources Planning and Systems Research Ltd, 278, 2002.

Essink, G., Van Baaren, E., and De Louw, P.: Effects of climate change on coastal groundwater systems: a modeling study in the Netherlands, Water Resources Research,

805 46, 2010.

Fleury, P., Bakalowicz, M., and de Marsily, G.: Submarine springs and coastal karst aquifers: a review, Journal of Hydrology, 339, 79-92, 2007.

Gallegos, J. J., Hu, B. X., and Davis, H.: Simulating flow in karst aquifers at laboratory and sub-regional scales using MODFLOW-CFP, Hydrogeology Journal, 21, 1749-1760,

810   2013.

Guo, W., and Langevin, C.: User's guide to SEWAT: a computer program for simulation of three-dimensional variable-density ground-water flow, Water Resources Investigations Report. United States Geological Survey, 2002.

Hill, M. C., and Tiedeman, C. R.: Effective groundwater model calibration: with analysis

815   of data, sensitivities, predictions, and uncertainty, John Wiley & Sons, 2006.

Inouchi, K., Kishi, Y., and Kakinuma, T.: The motion of coastal groundwater in response to the tide, Journal of Hydrology, 115, 165-191, 1990.

IPCC: Contribution of Working Groups I, II and III to the Fourth Assessment Report of the Intergovernmental Panel on Climate Change, Geneva, Switzerland, 104 pp., 2007.

820   Kaufmann, G., and Braun, J.: Karst aquifer evolution in fractured, porous rocks, Water Resources Research, 36, 1381-1391, 2000.

Kernagis, D. N., McKinlay, C., and Kincaid, T. R.: Dive Logistics of the Turner to Wakulla Cave Traverse, 2008.

Kincaid, T. R., and Werner, C. L.: Conduit Flow Paths and Conduit/Matrix Interactions

825   Defined by Quantitative Groundwater Tracing in the Floridan Aquifer, Sinkholes and the Engineering and Environmental Impacts of Karst: Proceedings of the Eleventh Multidisciplinary Conference, Am. Soc. of Civ. Eng. Geotech. Spec. Publ, 2008, 288-302,

Langevin, C. D., Shoemaker, W. B., and Guo, W.: MODFLOW-2000, the US Geological

830   Survey Modular Ground-Water Model--Documentation of the SEAWAT-2000 Version with the Variable-Density Flow Process (VDF) and the Integrated MT3DMS Transport Process (IMT), US Department of the Interior, US Geological Survey, 2003.

Martin, J. B., and Dean, R. W.: Exchange of water between conduits and matrix in the Floridan aquifer, Chemical Geology, 179, 145-165, 2001.

835   Martin, J. B., Gulley, J., and Spellman, P.: Tidal pumping of water between Bahamian blue holes, aquifers, and the ocean, Journal of Hydrology, 416, 28-38, 2012.

Moore, W. S., and Wilson, A. M.: Advective flow through the upper continental shelf driven by storms, buoyancy, and submarine groundwater discharge, Earth and Planetary Science Letters, 235, 564-576, 2005.

840 Morris, M. D.: Factorial sampling plans for preliminary computational experiments, Technometrics, 33, 161-174, 1991.

Poeter, E. P., and Hill, M. C.: Documentation of UCODE, a computer code for universal inverse modeling, DIANE Publishing, 1998.

Reimann, T., Liedl, R., Giese, M., Geyer, T., Maréchal, J.-C., Dörfliger, N., Bauer, S.,

845 and Birk, S.: Addition and Enhancement of Flow and Transport processes to the MODFLOW-2005 Conduit Flow Process, 2013 NGWA Summit—The National and International Conference on Groundwater, 2013,

Reimann, T., Giese, M., Geyer, T., Liedl, R., Maréchal, J.-C., and Shoemaker, W. B.: Representation of water abstraction from a karst conduit with numerical discrete-

850 continuum models, Hydrology and Earth System Sciences, 18, 227-241, 2014.

Saltelli, A., Tarantola, S., Campolongo, F., and Ratto, M.: Sensitivity analysis in practice: a guide to assessing scientific models, John Wiley & Sons, 2004.

Scanlon, B. R., Mace, R. E., Barrett, M. E., and Smith, B.: Can we simulate regional groundwater flow in a karst system using equivalent porous media models? Case study,

855 Barton Springs Edwards aquifer, USA, Journal of hydrology, 276, 137-158, 2003.

Shoemaker, W. B.: Important observations and parameters for a salt water intrusion model, Ground Water, 42, 829-840, 2004.

Shoemaker, W. B., Kuniansky, E. L., Birk, S., Bauer, S., and Swain, E. D.: Documentation of a conduit flow process (CFP) for MODFLOW-2005, 2008.

860 Voss, C. I., and Provost, A. M.: SUTRA, US Geological Survey Water Resources Investigation Reports, 84-4369, 1984.

Voss, C. I., and Souza, W. R.: Variable density flow and solute transport simulation of regional aquifers containing a narrow freshwater‐saltwater transition zone, Water Resources Research, 23, 1851-1866, 1987.

865 Werner, A. D., and Simmons, C. T.: Impact of sea‐level rise on sea water intrusion in coastal aquifers, Groundwater, 47, 197-204, 2009.

Werner, A. D., Bakker, M., Post, V. E., Vandenbohede, A., Lu, C., Ataie-Ashtiani, B., Simmons, C. T., and Barry, D. A.: Seawater intrusion processes, investigation and management: recent advances and future challenges, Advances in Water Resources, 51, 3-26, 2013.

WHO: Guidelines for Drinking-water Quality, 104-108, 2011.

Wilson, A. M., Moore, W. S., Joye, S. B., Anderson, J. L., and Schutte, C. A.: Storm‐driven groundwater flow in a salt marsh, Water Resources Research, 47, 2011.

Xu, Z., Hu, B. X., Davis, H., and Cao, J.: Simulating long term nitrate-N contamination processes in the Woodville Karst Plain using CFPv2 with UMT3D, Journal of Hydrology, 524, 72-88, 2015a.

Xu, Z., Hu, B. X., Davis, H., and Kish, S.: Numerical study of groundwater flow cycling controlled by seawater/freshwater interaction in a coastal karst aquifer through conduit network using CFPv2, Journal of contaminant hydrology, 182, 131-145, 2015b.

Xu, Z., Bassett, S. W., Hu, B., and Dyer, S. B.: Long distance seawater intrusion through a karst conduit network in the Woodville Karst Plain, Florida, Scientific Reports, 6, 2016.

Xu, Z., and Hu, B. X.: Development of a discrete‐continuum VDFST‐CFP numerical model for simulating seawater intrusion to a coastal karst aquifer with a conduit system, Water Resources Research, 53, 688-711, 10.1002/2016WR018758., 2017.

Table 1. The symbols and definitions of parameters used in this study, the specified evaluated values in local sensitivity study and evaluation ranges (the lower and upper constraints) of each parameter in global sensitivity analysis.

Parameter	Definitions	Lower	Upper	Evaluated value	Unit
HY_P	Hydraulic conductivity (porous medium)	1.524	4.572	2.286	$(\times 10^3)$ meters/day
HY_C	Hydraulic conductivity (conduit)	3.048	9.144	6.096	$(\times 10^5)$ meters/day
SS_P	Specific storage (porous medium)	4.00	6.00	5.00	$(\times 10^{-7})$ dimensionless
SS_C	Specific storage (conduit)	0.03	0.07	0.05	dimensionless
RCH	Recharge rate on the surface	0.00	0.03	0.01	meters/day
H_SL	Sea level at the submarine spring	-0.305	0.914	0.305	meters
PO_P	Porosity (porous medium)	0.001	0.005	0.003	dimensionless
PO_C	Porosity (conduit)	0.200	0.400	0.300	dimensionless
SC	Salinity at the submarine spring	0.0	35.0	35.0	PSU
DISP_P	Longitudinal dispersivity (porous medium)	6.10	12.20	10.00	meters
DISP_C	Longitudinal dispersivity (conduit)	0.15	0.60	0.30	meters
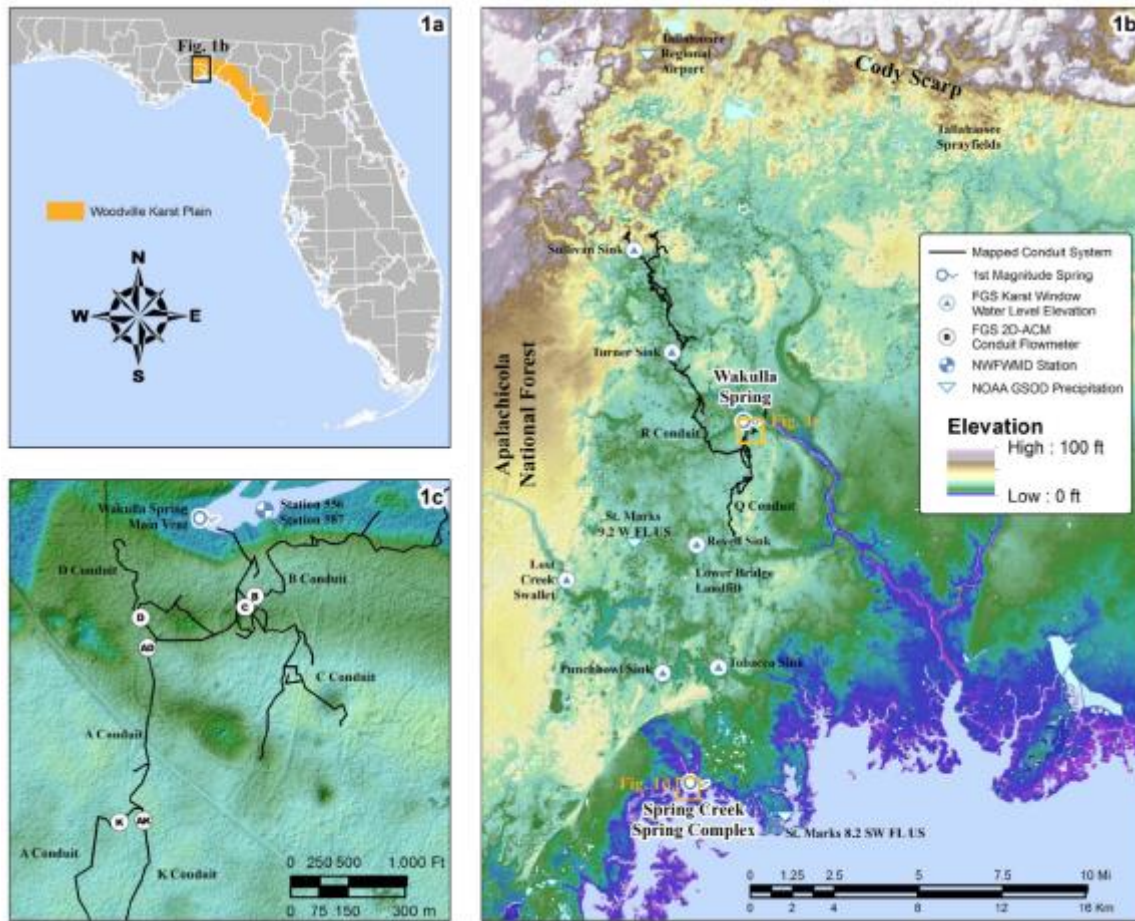
Figure 1. a) Locations of the Woodville Karst Plain (WKP) and the study site; b) The map of the Woodville Karst Plain showing the locations of features of note with the study; c) The detail of cave system near Wakulla Springs. Modified from Xu et al., (2016).
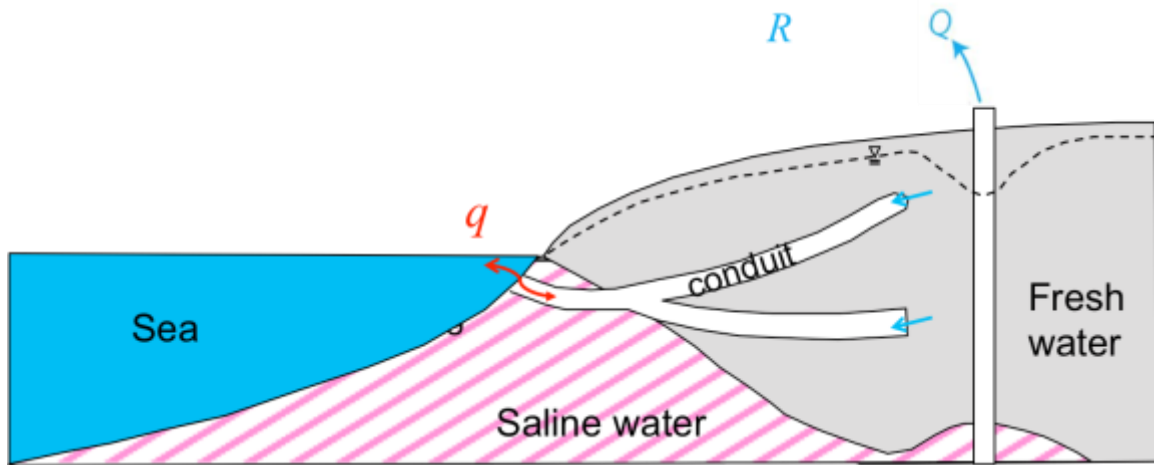
Figure 2. Schematic figure of a coastal karst aquifer with conduit networks and a submarine spring opening to the sea in a cross section. Flow direction q would be seaward when sea level drops, pumping rate Q is low and precipitation recharge R is large; however, reversal flow occurs when sea level rises, pumping rate Q is high or precipitation recharge R is small.

1   22   139 140
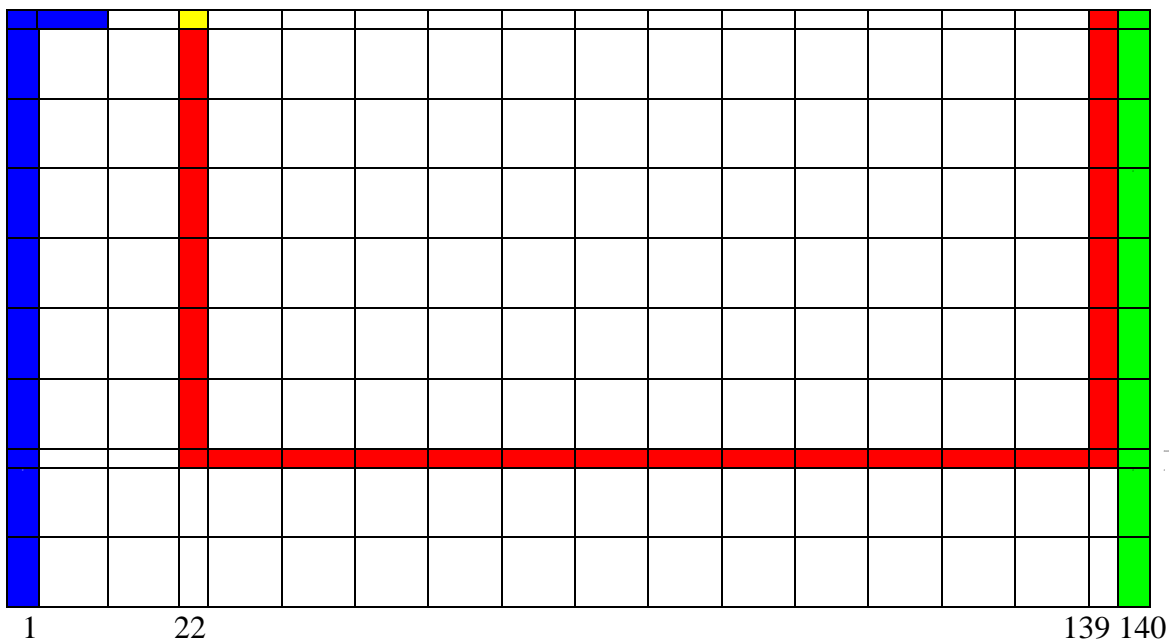
Explanations:

Constant head and constant concentration of the submarine spring and outlet of karst conduit system, however, various in different cases of numerical models

Sea-edge boundary: constant head (0.0 ft in normal sea level case) and constant concentration (35 PSU)

Inland boundary: constant head (5.0 ft) and constant concentration (0 PSU)

Conduit: high hydraulic conductivity, porosity and specific storage

Porous medium: low hydraulic conductivity, porosity and specific storage

Figure 3. Schematic figure of finite difference grid discretization and boundary conditions applied in the SEAWAT model. Every cell represents 10 horizontal cells and 4 vertical cells, except the boundary and conduit layer in color with smaller width. The submarine spring is located at column #22, layer #1, and the inland spring is located at column #139, layer #1. The conduit system starts from the top of column #22, descends downward to layer #29, horizontally extends to column #139, and then rises upward to the top through column #139.
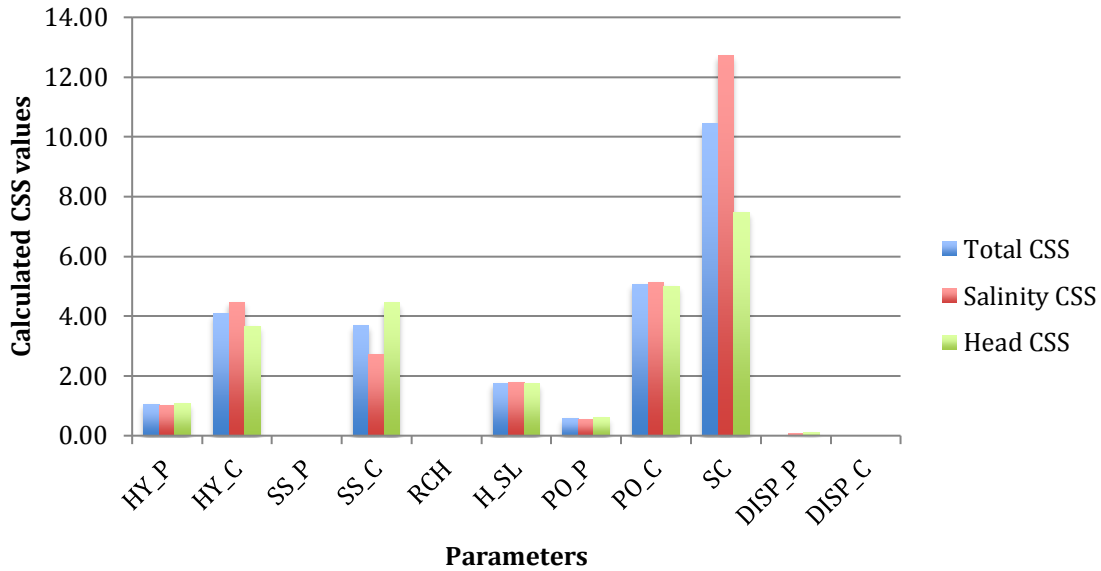
Figure 4. The CSSs (Composite Scaled Sensitivities) of all parameters with respect to simulations in the conduit (layer #29) in the local sensitivity analysis.
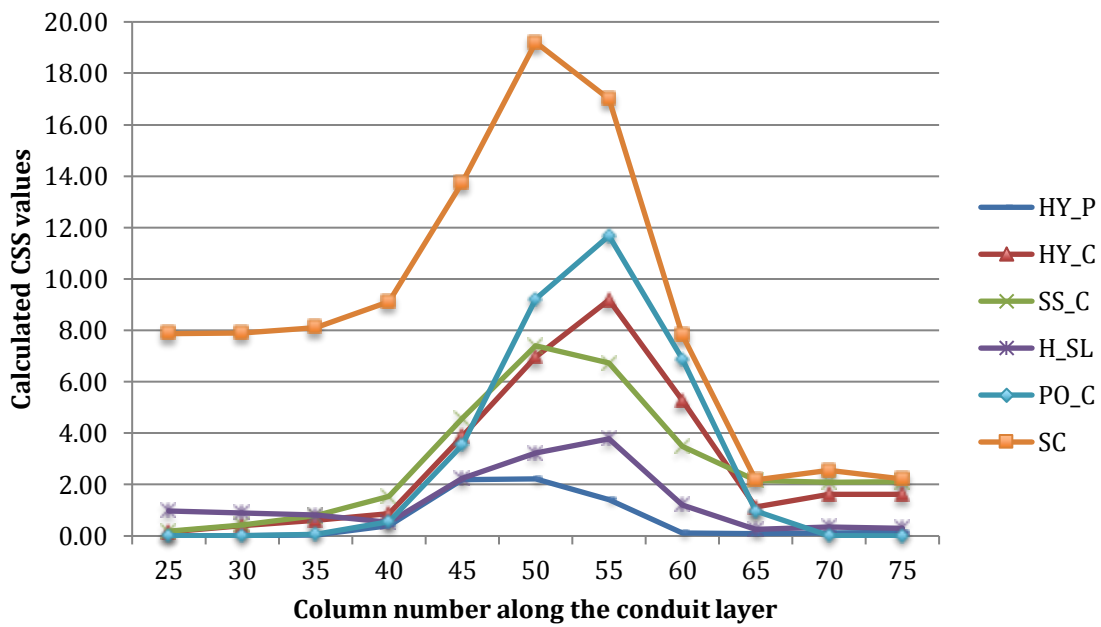
Figure 5. The CSSs (Composite Scaled Sensitivities) of selected parameters at different locations along the conduit layer (from column #25 to column #75) in the local sensitivity analysis.
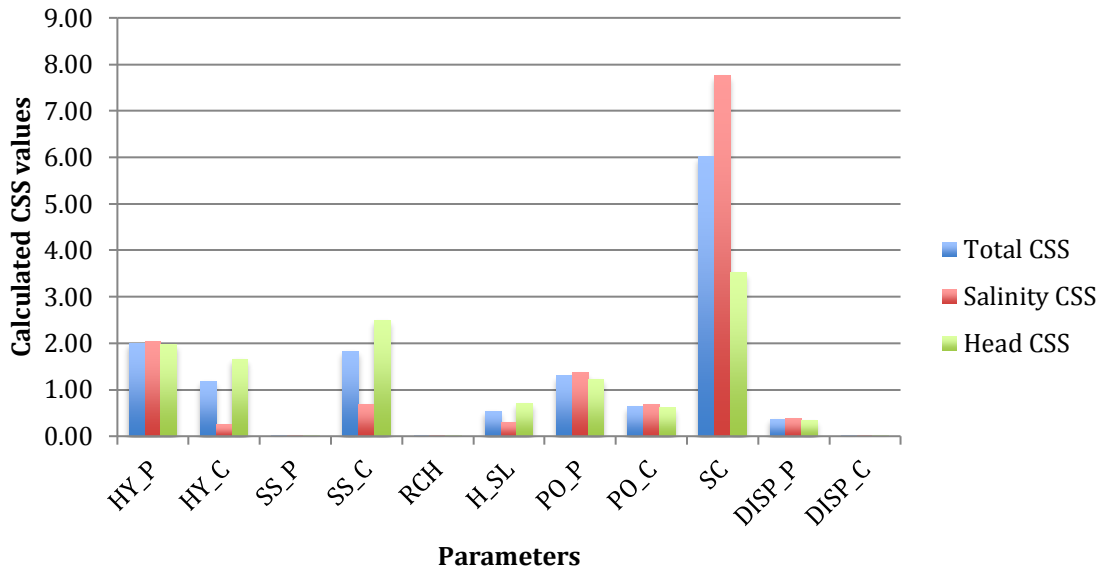
Figure 6. The CSSs (Composite Scaled Sensitivities) of all parameters with respect to simulations in the porous medium (layer #24) in the local sensitivity analysis.
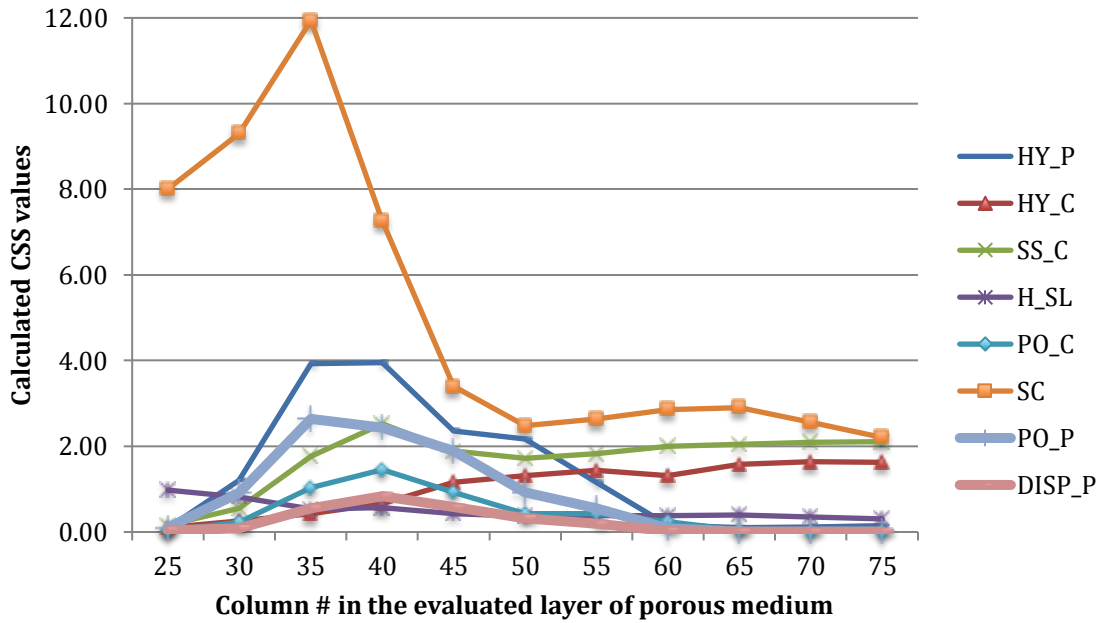
Figure 7. The CSSs (Composite Scaled Sensitivities) at different locations in the porous medium (from column #25 to column #75 at layer # 24) in the local sensitivity analysis.
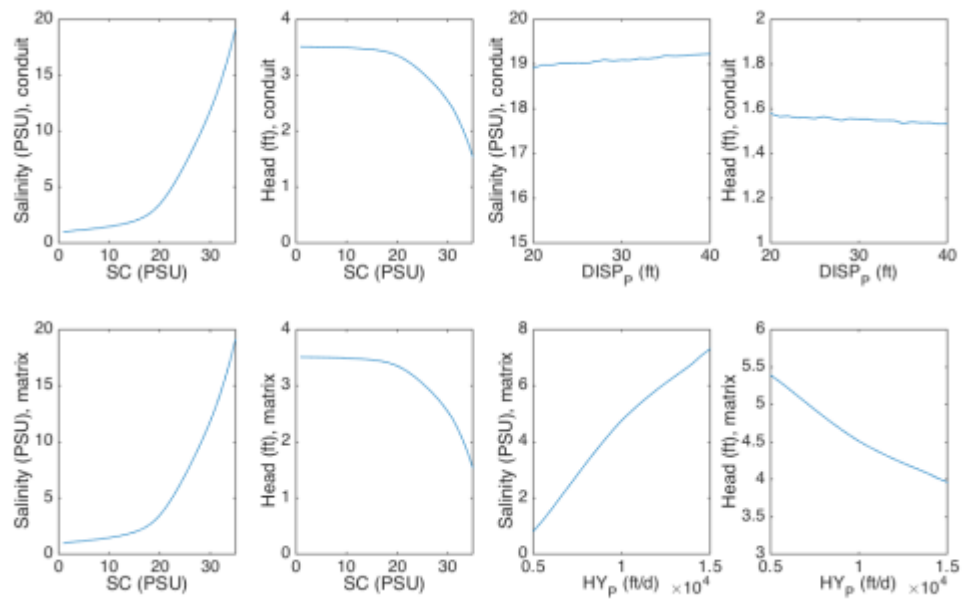
Figure 8. The non-linear relationship between head and salinity simulations with respect to parameters SC, DISP_P and HY_P. (Note that the scale for each plot is different).
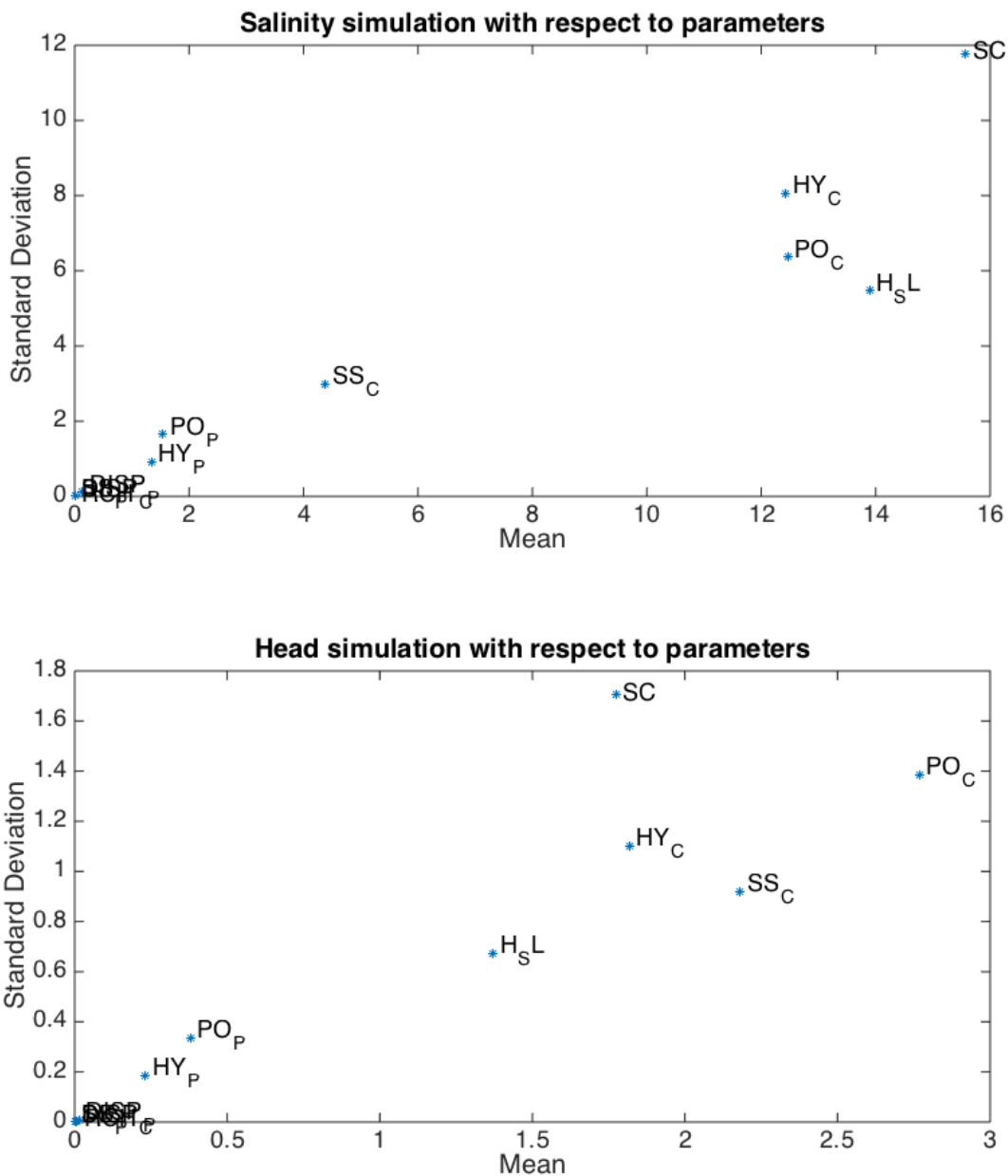
Figure 9. Mean and standard deviation of the EEs (elementary effects) of parameters with respect to simulations in the conduit (column #50, layer #29) in the global sensitivity analysis by Morris method: a) salinity simulation (top); b) head simulation (bottom).
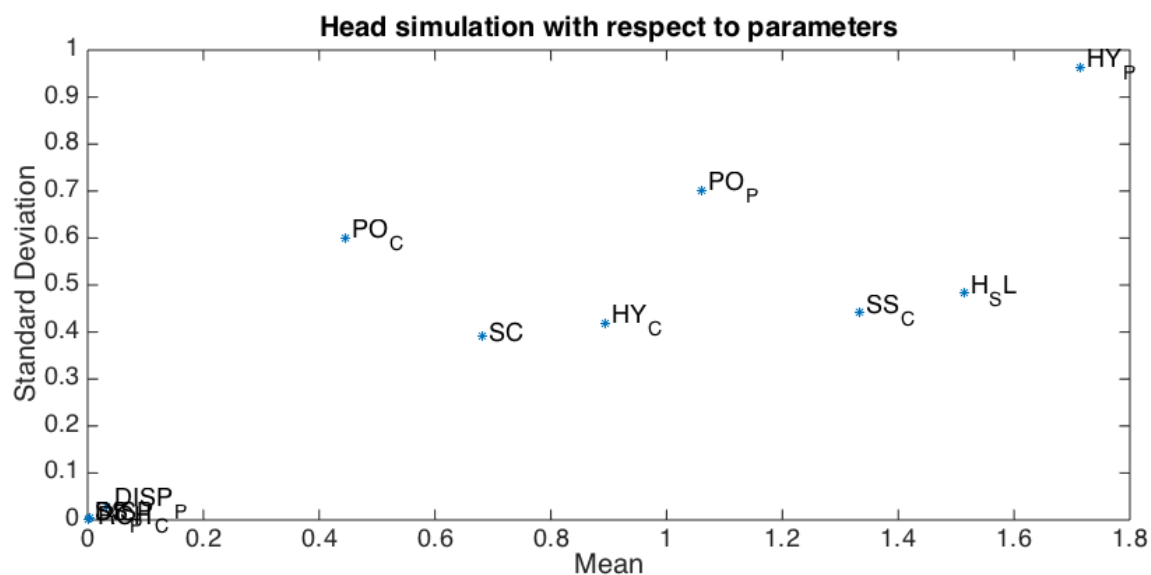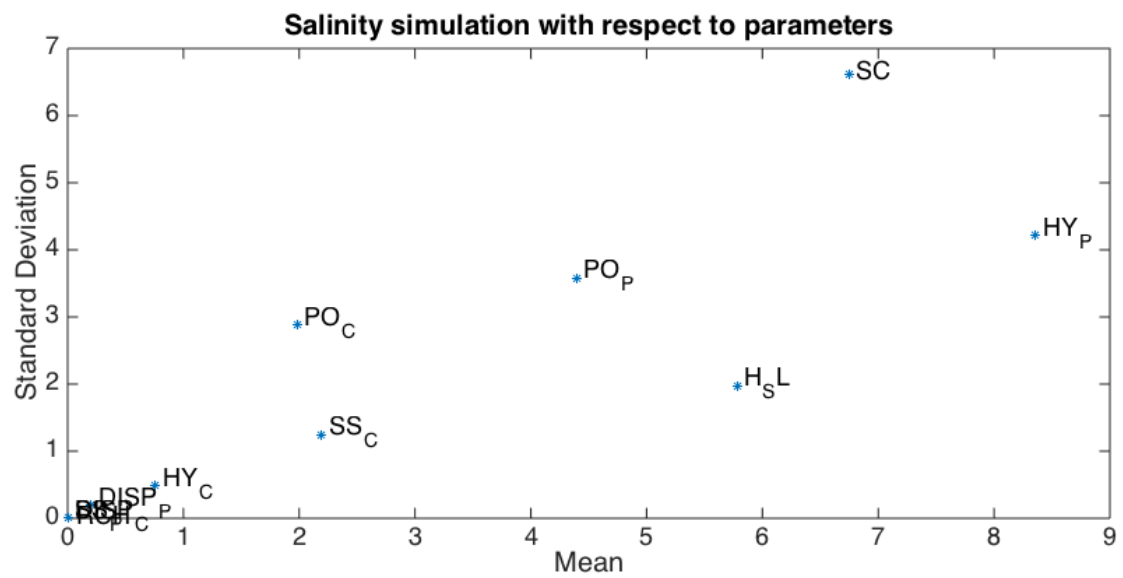
Figure 10. Mean and standard deviation of the EEs (elementary effects) of parameters with respect to simulations in the porous medium (column #35, layer #24) in the global sensitivity analysis by Morris method: a) salinity simulation (top); b) head simulation (bottom).
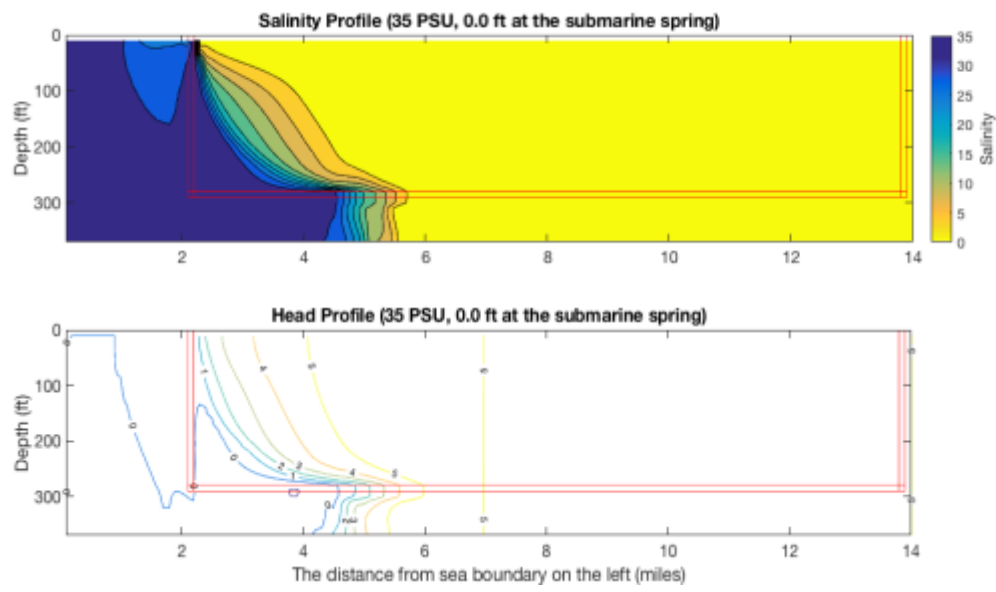
Figure 11. Salinity (top) and head (bottom) simulations of the maximum seawater intrusion benchmark case (35 PSU, 0.0 ft at the submarine spring).
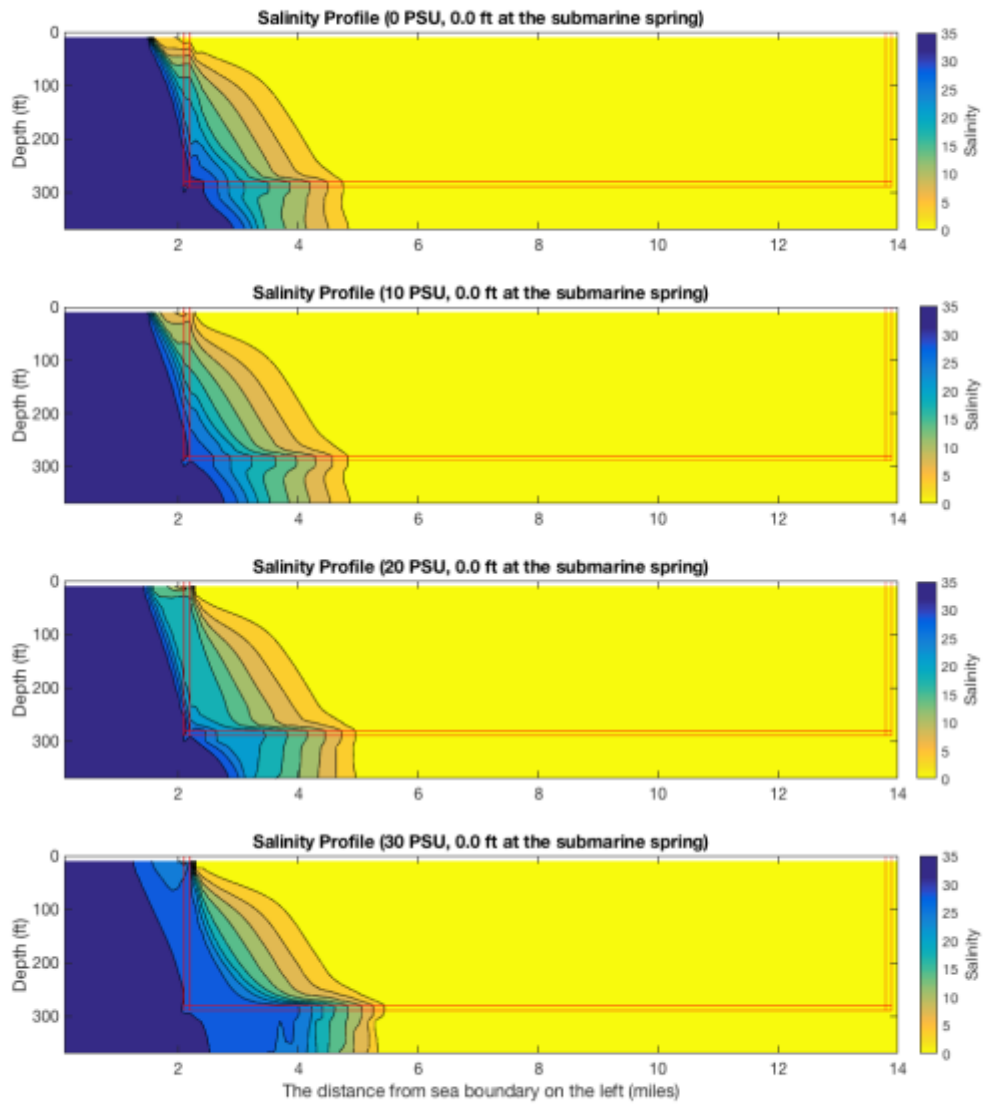
Figure 12. Salinity simulation of seawater intrusion with various salinity at the submarine spring, indicating different rainfall recharge and freshwater discharge conditions: A) 0.0 PSU, 0.0 ft at the submarine spring; B) 10.0 PSU, 0.0 ft at the submarine spring; C) 20.0 PSU, 0.0 ft at the submarine spring; D) 30.0 PSU, 0.0 ft at the submarine spring (from top to bottom).
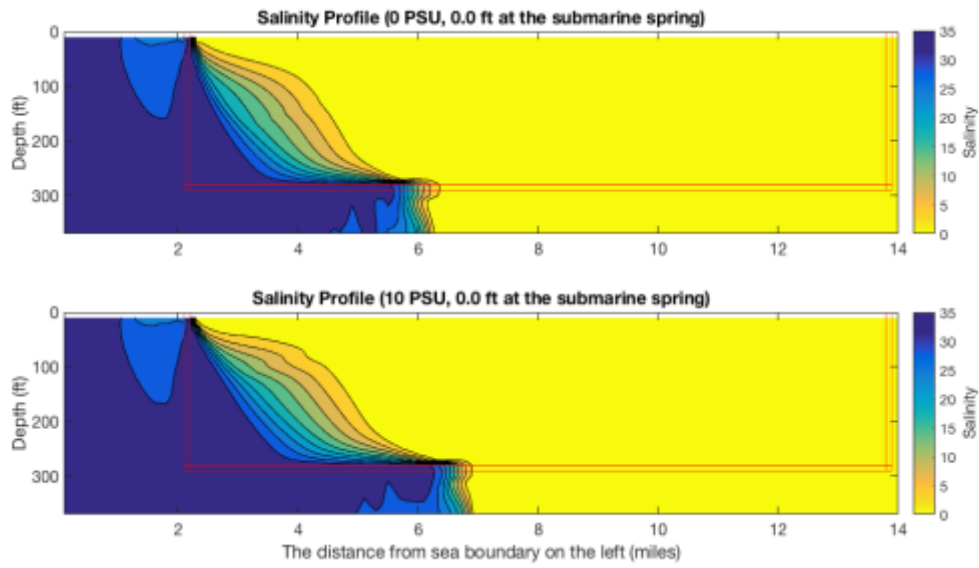
Figure 13. Salinity simulation of seawater intrusion with various sea level conditions: A) 35.0 PSU, 3.0 ft at the submarine spring; B) 35.0 PSU, 6.0 ft at the submarine spring (from top to bottom).
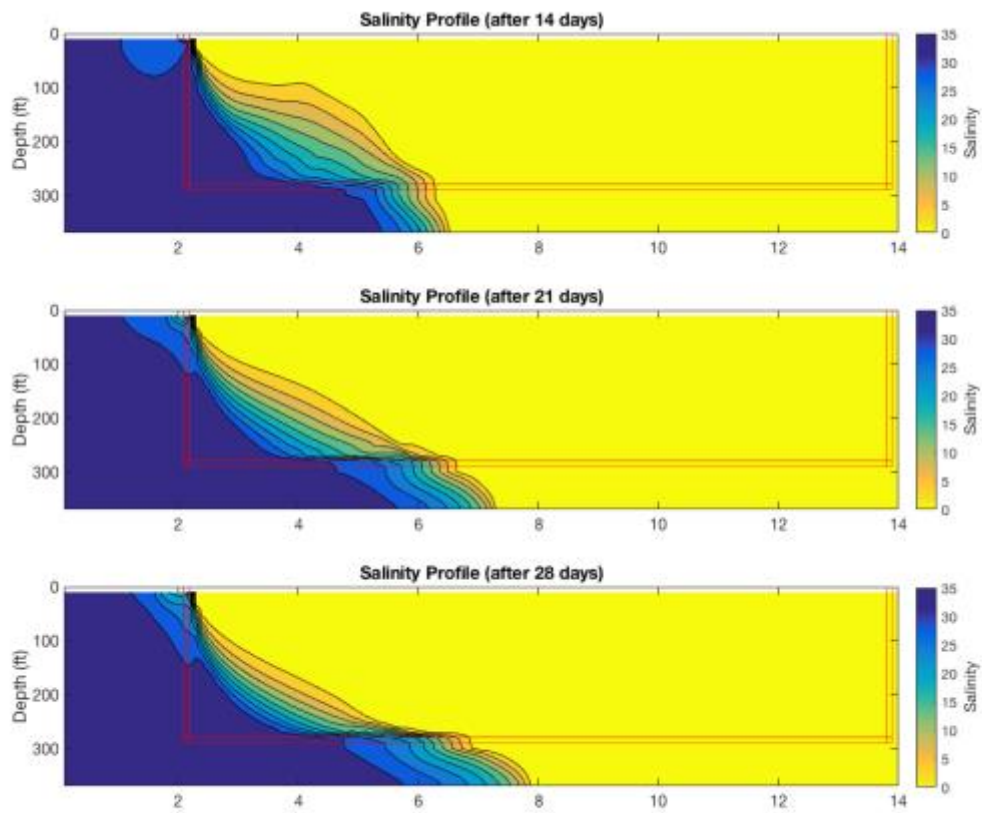
Figure 14. Salinity simulation of the maximum seawater intrusion benchmark case (35 PSU, 0.0 ft at the submarine spring) with extend simulation time during a low rainfall period: A) 14-day simulation period; B) 21-day simulation period; C) 28-day simulation period (from top to bottom).